ATTACHMENT 3

Areva Calculation, "Byron/Braidwood RVCH Nozzle IDTB Repair Weld Anomaly 32-9244389-000", Revision 0

NON- PROPRIETARY

AREVA

CALCULATION SUMMARY SHEET (CSS)

Document No. 32 - 9244389 - 000 Safety Related: ☒Yes ☐ No

Title Byron/Braidwood RVCH Nozzle IDTB Repair Weld Anomaly – Non Proprietary

PURPOSE AND SUMMARY OF RESULTS:

Purpose:

The purpose of this analysis is to perform fracture mechanics evaluation of a postulated anomaly in the Exelon Byron Units 1 and 2 and Braidwood Units 1 and 2 (Byron/Braidwood) Reactor Vessel Closure Head (RVCH) Control Rod Drive Mechanisms (CRDM) / Reactor Vessel Level Indication Systems (RVLIS) / Core Exit Thermocouple (CETC) Nozzles contingency modification. According to the design specification document, Reference [8.2], this anomaly is postulated to be a 0.1 inch flaw extending 360 degrees around the circumference at the "triple point" locations where there is a confluence of three materials; the RVCH low alloy steel base material, the SB-167 Alloy 600 existing nozzle or SB-166 Alloy 690 replacement nozzle, and the [ ] weld material. Several potential flaw propagation paths are considered in the flaw evaluations. Flaw acceptance is based on the ASME B&PV Code, 2001 with 2002 & 2003 Addenda, Section XI criteria for applied stress intensity factor (IWB-3612) and limit load (IWB-3642), Reference [8.1].

Results:

The results of the analyses demonstrate that the 0.10 inch weld anomaly is acceptable for a 40 year design life of the Byron/Braidwood CRDM/RVLIS/CETC Nozzle Repair. The minimum fracture toughness margins for flaw propagation Paths 3a/b/c and 4a/b/c have been shown to be acceptable as compared to the required margins of $\sqrt{10}$ for normal/upset conditions and $\sqrt{2}$ for emergency/faulted/test conditions per Section XI, IWB-3612 of Reference [8.1].

A limit load analysis was performed considering the ductile weld repair material along flaw propagation Paths 1a/b/c & 2a/b/c. The analysis showed that for the postulated circumferential flaw the minimum margin on allowable stress is [ ] For the axial flaw the minimum margin on allowable flaw depth is [ ] Fracture toughness margins have also been demonstrated for the postulated cylindrical flaws. Also for the cylindrical flaws it is shown that the applied shear stress at the remaining ligament is less than the allowable shear stress per NB-3227.2, Reference [8.10].

This document contains a total of 52 pages including pages 1-50 and Appendix A (2 pages).

If the computer software used herein is not the latest version per the EASI list, AP 0402-01 requires that justification be provided.

THE FOLLOWING COMPUTER CODES HAVE BEEN USED IN THIS DOCUMENT:

CODE/VERSION/REV	CODE/VERSION/REV
AREVACGC 5.0	

THE DOCUMENT CONTAINS ASSUMPTIONS THAT SHALL BE VERIFIED PRIOR TO USE

☐Yes

☒ No

Review Method: ☒ Design Review (Detailed Check)

☐ Alternate Calculation

Signature Block

Name and Title (printed or typed)	Signature	P/R/A and LP/LR	Date	Pages/Sections Prepared/Reviewed/Approved
Silvester J. Noronha Principal Engineer	SJ Noronha	P	7/29/15	All
Tom Riordan Engineer IV	T Ehr	R	29 JUL 2015	All
Tim Wiger, Manager	T.M. Wiger	A	7/29/15	All

Notes: P/R/A designates Preparer (P), Reviewer (R), Approver (A);
LP/LR designates Lead Preparer (LP), Lead Reviewer (LR)

In reviewing and approving the initial release (Rev. 000), the lead reviewer/approver shall designate 'All' in pages/sections reviewed/approved.

In reviewing and approving revisions, the lead preparer and lead reviewer shall use 'All' in the pages/sections reviewed/approved. 'All' means that the changes and the effect of the changes on the entire document have been reviewed/approved. It does not mean that the lead reviewer/approver has reviewed/approved all the pages of the document.

Project Manager Approval of Customer References (N/A if not applicable)

Name (printed or typed)	Title (printed or typed)	Signature	Date
N/A			

Record of Revision

Revision No.	Pages/Sections/Paragraphs Changed	Brief Description / Change Authorization
000	All	Initial Release

Table of Contents

Page

SIGNATURE BLOCK 2

RECORD OF REVISION 3

LIST OF TABLES 6

LIST OF FIGURES 7

1.0 PURPOSE AND SCOPE 8

2.0 METHODOLOGY 9
- 2.1 Postulated Flaws 9
- 2.2 Stress Intensity Factor (SIF) Solutions 10
- 2.3 Fatigue Crack Growth Laws 12
- 2.4 Fatigue Crack Growth Calculations 14
- 2.5 Acceptance Criteria 14

3.0 ASSUMPTIONS 16
- 3.1 Unverified Assumptions 16
- 3.2 Justified Assumptions 16
- 3.3 Modelling Simplifications 16

4.0 DESIGN INPUTS 17
- 4.1 Geometry 17
- 4.2 Material Strength 17
- 4.3 Fracture Toughness 18
- 4.4 Applied Stresses Intensity Factor Calculation 18

5.0 CALCULATIONS 22
- 5.1 Circumferential Flaw for Paths 1a/b/c & 2a/b/c 22
- 5.2 Axial Flaw for Paths 1a/b/c & 2a/b/c 25
- 5.3 Cylindrical Flaw for Paths 3a/b/c & 4a/b/c 30

6.0 RESULTS 45
- 6.1 Fatigue Crack Growth of Continuous External Circumferential Flaw 45
- 6.2 Fatigue Crack Growth of Semi-Circular External Axial Flaw 45
- 6.3 Fatigue Crack Growth of Continuous Cylindrical Flaw along Paths 3a & 4a 45
- 6.4 Fatigue Crack Growth of Continuous Cylindrical Flaw along Paths 3b & 4b 46
- 6.5 Fatigue Crack Growth of Continuous Cylindrical Flaw along Paths 3c & 4c 47

7.0 COMPUTER USAGE 48
- 7.1 Validation 48

Table of Contents
(continued)

Page

7.2 Computer Files 48

8.0 REFERENCES 50

APPENDIX A : VERIFICATION OF SIF FOR CYLINDRICAL FLAW A-1

List of Tables

Page

Table 4-1 - Material Strength 18
Table 4-2 – Operating Transients and Cycles 19
Table 4-3 – Replacement Nozzle Internal Mechanical Loads 20
Table 4-4 – Axial Stresses due to Seismic Loads 21
Table 5-1 – Crack Growth for 360° Circumferential Flaw (Paths 1a/b/c and 2a/b/c) 22
Table 5-2 – Individual Transient Contribution to Crack Growth for 360° Circumferential Flaw (Paths 1a/b and 2a/b) 23
Table 5-3 – Individual Transient Contribution to Crack Growth for 360° Circumferential Flaw (Paths 1c and 2c) 24
Table 5-4 – End of Life Evaluation for Continuous External Circumferential Flaw (Limit Load) 25
Table 5-5 – Radial Crack Growth for Axial Flaw 25
Table 5-6 – Axial Crack Growth for Axial Flaw 25
Table 5-7 – Individual Transient Contribution to Radial Crack Growth for Axial Flaw (Paths 1a/b and 2a/b) 26
Table 5-8 – Individual Transient Contribution to Axial Crack Growth for Axial Flaw (Paths 1a/b and 2a/b) 27
Table 5-9 – Individual Transient Contribution to Radial Crack Growth for Axial Flaw (Paths 1c and 2c) 28
Table 5-10 – Individual Transient Contribution to Axial Crack Growth for Axial Flaw (Paths 1c and 2c) 29
Table 5-11 – End of Life Evaluation for External Axial Flaw (Limit Load) 30
Table 5-12 – First Year Crack Growth for Cylindrical Flaw along Path 3a (Bottom Corner) 31
Table 5-13 – First Year Crack Growth for Cylindrical Flaw along Path 3b (Bottom Corner) 32
Table 5-14 – First Year Crack Growth for Cylindrical Flaw along Path 3c (Bottom Corner) 33
Table 5-15 – First Year Crack Growth for Cylindrical Flaw along Path 4a (Bottom Corner) 34
Table 5-16 – First Year Crack Growth for Cylindrical Flaw along Path 4b (Bottom Corner) 35
Table 5-17 – First Year Crack Growth for Cylindrical Flaw along Path 4c (Bottom Corner) 36
Table 5-18 – First Year Crack Growth for Cylindrical Flaw along Path 3a (Top Corner) 37
Table 5-19 – First Year Crack Growth for Cylindrical Flaw along Path 3b (Top Corner) 38
Table 5-20 – First Year Crack Growth for Cylindrical Flaw along Path 3c (Top Corner) 39
Table 5-21 – First Year Crack Growth for Cylindrical Flaw along Path 4a (Top Corner) 40
Table 5-22 – First Year Crack Growth for Cylindrical Flaw along Path 4b (Top Corner) 41
Table 5-23 – First Year Crack Growth for Cylindrical Flaw along Path 4c (Top Corner) 42
Table 5-24 – Final Crack Depth for Cylindrical Flaw (Bottom Corner) 42
Table 5-25 – Final Crack Depth for Cylindrical Flaw (Top Corner) 42
Table 5-26 – LEFM Margin for Cylindrical Flaw 44
Table 7-1 – Computer Files for Crack Growth Evaluation 49

List of Figures

Page

Figure 2-1 – Illustration of Crack Propagation Paths 10
Figure 2-2 – OD, Partial Through-Wall, 360° Circumferential Flaw 11
Figure 2-3 – OD, Partial Through-Wall, Semi-Elliptical Axial Flaw 11

1.0 PURPOSE AND SCOPE

As required by the Design Specification document, Reference [8.2], the purpose of this analysis is to perform fracture mechanics evaluation of a postulated anomaly in the Exelon Byron Units 1 and 2 and Braidwood Units 1 & 2 (Byron/Braidwood) Reactor Vessel Closure Head (RVCH) Control Rod Drive Mechanisms (CRDM) / Reactor Vessel Level Indication Systems (RVLIS) / Core Exit Thermocouple (CETC) Nozzle contingency modification.

Per Reference [8.2], this anomaly is postulated to be a 0.1 inch flaw extending 360 degrees around the circumference at the "triple point" locations where there is a confluence of three materials; the RVCH low alloy steel base material, the SB-167 Alloy 600 existing nozzle or SB-166 Alloy 690 replacement nozzle, and the [ ] weld material. Several potential flaw propagation paths are considered in the flaw evaluations. Flaw acceptance is based on the ASME B&PV Code, 2001 with 2002 & 2003 Addenda, Section XI criteria for applied stress intensity factor (IWB-3612) and limit load (IWB-3642), Reference [8.1].

The repair scope includes potential nozzle modifications at any of the Control Rod Drive Mechanisms (CRDM), the Reactor Vessel Level Indication Systems (RVLIS) and/or the Core Exit Thermocouple (CETC). Therefore, the Section XI analysis must bound all CRDM, RVLIS, and CETC locations on the RVCH. Per Reference [8.3], the CETC Nozzle is considered to be the controlling component, and therefore, this analysis will consider the CETC Nozzle only.

The present fracture mechanics analysis provides justification, in accordance with Section XI of the ASME B&PV Code, Reference [8.1], for operating with the postulated weld anomaly at the upper and lower triple point locations defined for the CETC nozzle. Predictions of fatigue crack growth are based on the original design life of 40 years, Reference [8.4].

2.0 METHODOLOGY

This section presents several aspects of linear elastic fracture mechanics (LEFM) and limit load analysis (used to address the ductile weld materials) that form the basis of the present flaw evaluation.

2.1 Postulated Flaws

The triple point weld anomaly is postulated to be semi-circular in shape with an initial depth of 0.1", as indicated in Reference [8.2]. It is further assumed that the anomaly extends 360° around the new repair weld.

The anomaly could be located in the upper and lower triple point regions, the regions are called "triple point" since three materials intersect at these locations. The materials are:

- The existing nozzle material, SB-167 – Alloy 600 (Upper Triple Point) or the replacement nozzle material, SB-166 – Alloy 690 (Lower Triple Point), Reference [8.2].
- The new weld filler material, [ ] Reference [8.2].
- The RV closure head material, SA-533 Grade B Class 1, Reference [8.2].

Three flaw types are postulated to simulate various orientations and propagation directions for the weld anomaly. A circumferential flaw and an axial flaw at the outside surface of the new weld would both propagate in the horizontal direction toward the inside surface of the new weld. The cylindrically oriented flaws along the interface between the weld and RV closure head would propagate downward between the two components from the top flaw tip and upward between the two components from the bottom flaw tip. The horizontal and vertical flaw propagation directions are represented in Figure 2-1, Reference [8.3], by separate paths for the downhill and uphill sides of the Nozzle, as discussed below. For both these directions, fatigue crack growth will be calculated.

Horizontal Direction (Paths 1a/b/c and 2a/b/c):

Flaw propagation is across the Nozzle IDTB Weld wall thickness from the OD to the ID of the IDTB Weld. These are the shortest paths through the component wall passing through the new [ ] weld material at the upper (Paths 1a, 1b and 1c) and lower triple points (Paths 2a, 2b, and 2c), Reference [8.2].

For completeness, two types of flaws are postulated at the outside surface of the tube. A 360° continuous circumferential flaw, lying in a horizontal plane, is considered to be a conservative representation of crack-like defects that may exist in the weld anomaly. This flaw would be subjected to axial stresses in the tube. An axially oriented semi-circular outside surface flaw is also considered since it would lie in a plane that is normal to the higher circumferential stresses. Both of these flaws would propagate toward the inside surface of the tube.

Vertical Direction (Paths 3a/b/c and 4a/b/c):

Flaw propagation is at the outside surface of the repair weld between the weld and the RVCH. A continuous surface flaw is postulated to lie along this cylindrical interface between the two materials. This flaw, driven by radial stresses, may propagate along either the new [ ] weld material or the SA-533, Gr. B RVCH material from either corner (top or bottom). Flaws along Paths 3a, 3b, and 3c are postulated in the weld and flaws along Paths 4a, 4b, and 4c are postulated in the RVCH.

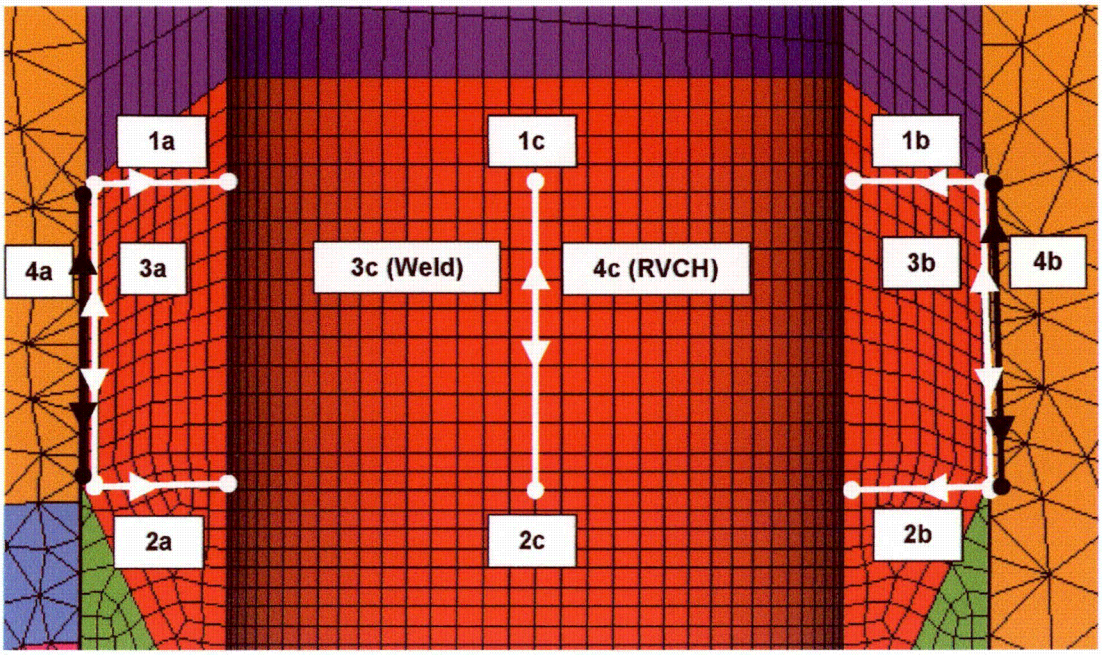

Figure 2-1 – Illustration of Crack Propagation Paths

2.2 Stress Intensity Factor (SIF) Solutions

Three flaw types are postulated for the current evaluation of the weld anomaly defect at the triple points. For paths 1a/b/c and 2a/b/c both 360° circumferential and axial surface flaws at the OD of the IDTB weld are postulated. The solutions for both types of flaws are available in the AREVACGC code, Reference [8.5], which implements the Stress Intensity Factor (SIF) evaluation for these types of flaws using the weight function method. AREVACGC performs the fatigue crack growth calculations. The schematics for both the 360° circumferential and axial flaws postulated at the OD of the IDTB weld are illustrated in Figure 2-2 and Figure 2-3, respectively.

For the vertical paths (3a/b/c and 4a/b/c), a cylindrical flaw is postulated along the interface between the new repair weld and the RV head material. The potential for flaw propagation along this interface is likely if radial stresses are significant between the weld and head. This assessment utilizes an SIF solution for a continuous surface crack in a flat plate from Appendix A Section XI of the ASME B&PV Code, Reference [8.1]. Flat plate solutions are routinely used to evaluate flaws in cylindrical components such as the repair weld. The flat plate solution is inherently conservative for this application since the added constraint provided by the cylindrical structure reduces the crack opening displacements. Crack growth analysis is performed considering propagation through the [ ] weld metal or the low alloy steel RVCH material. To facilitate the calculation of the SIF for the cylindrical flaw, a visual basic code, KIeff_edge, was developed based on the theory in Appendix A Section XI of the ASME B&PV Code, Reference [8.1]. Appendix A of this document provides verification of the KIeff_edge visual basic function against hand calculations.

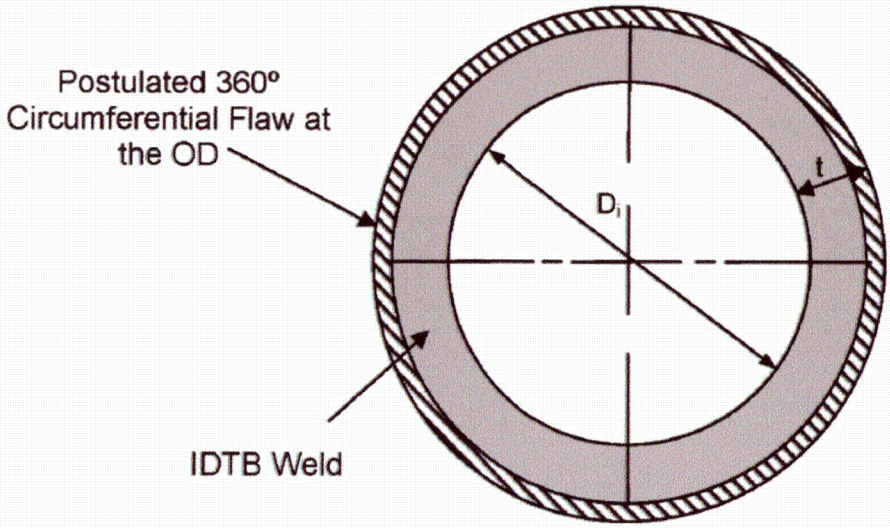

Figure 2-2 – OD, Partial Through-Wall, 360° Circumferential Flaw

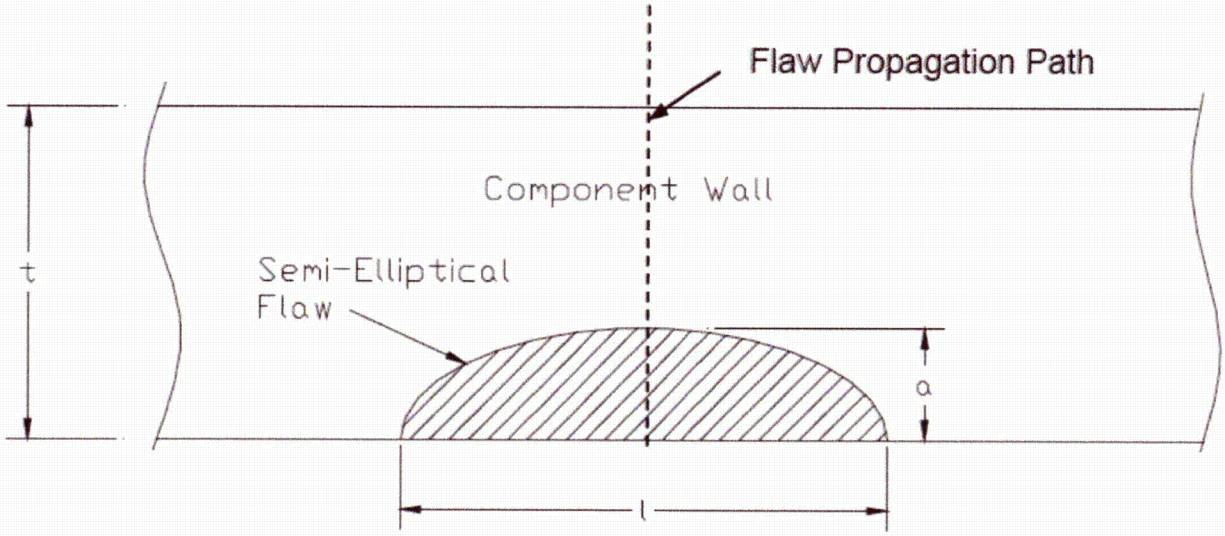

Where,

a = initial flaw depth
$l = 2a$ = flaw length
t = thickness

Figure 2-3 – OD, Partial Through-Wall, Semi-Elliptical Axial Flaw

2.3 Fatigue Crack Growth Laws

Flaw growth due to fatigue is characterized by

$$\frac{da}{dN} = C_o(\Delta K_I)^n$$

Where C_o and n are constants that depend on the material and environmental conditions, ΔK_I is the range of applied stress intensity factor in terms of ksi√in, and da/dN is the incremental flaw growth in terms of inches/cycle. For the embedded weld anomaly considered in the present analysis at the upper triple point, it is appropriate to use crack growth rates for an air environment. For the embedded weld anomaly considered at the lower triple point, the crack growth rates for material exposed to light-water reactor environments is utilized. Fatigue crack growth is also dependent on the ratio of the minimum to the maximum stress intensity factor; i.e.,

$$R = K_{min}/K_{max}$$

SA-533 Grade B Low Alloy Steel Material (RVCH)

From Article A-4300 of the 2001 Edition with 2002 through 2003 Addenda of Section XI, Reference [8.1], the fatigue crack growth constants for flaws in an air environment are:

$n = 3.07$
$C_o = 1.99 \times 10^{-10}\,S$

S is a scaling parameter to account for the R ratio and is given by $S = 25.72\,(2.88 - R)^{-3.07}$, where $0 \le R \le 1$ and $\Delta K_I = K_{max} - K_{min}$. For $R < 0$, ΔK_I depends on the crack depth, a, and the flow stress, σ_f. The flow stress is defined by $\sigma_f = ½(\sigma_{ys} + \sigma_{ult})$, where σ_{ys} is the yield strength and σ_{ult} is the ultimate tensile strength. For $-2 \le R \le 0$ and $K_{max} - K_{min} \le 1.12\,\sigma_f\sqrt{\pi a}$, S=1 and $\Delta K_I = K_{max}$. For $R < -2$ and $K_{max} - K_{min} \le 1.12\,\sigma_f\sqrt{\pi a}$, S = 1 and $\Delta K_I = (1 - R)\,K_{max}/3$. For $R < 0$ and $K_{max} - K_{min} > 1.12\,\sigma_f\sqrt{\pi a}$, S = 1 and $\Delta K_I = K_{max} - K_{min}$.

From Article A-4300, Reference [8.1], for material exposed to light-water reactor environments, the fatigue crack growth constants are:

$\Delta K_I = K_{max} - K_{min}$.

$0 \le R \le 0.25$, $\Delta K_I < 17.74$

$n = 5.95$
$S = 1.0$
$C_0 = 1.02 \times 10^{-12} S$

$\Delta K_I \ge 17.74$

$n = 1.95$
$S = 1.0$
$C_0 = 1.01 \times 10^{-7} S$

$0.25 < R < 0.65$, $\Delta K_I < 17.74\,[(3.75R + 0.06)/(26.9R - 5.725)]^{0.25}$

$n = 5.95$
$S = 26.9S - 5.725$
$C_0 = 1.02 \times 10^{-12} S$

$\Delta K_I \ge 17.74[(3.75R + 0.06)/(26.9R - 5.725)]^{0.25}$

		$n = 1.95$ $S = 3.75R + 0.06$ $C_0 = 1.01 \times 10^{-7}S$
$0.65 \leq R \leq 1.00$,	$\Delta K_I < 12.04$	
		$n = 5.95$ $S = 11.76$ $C_0 = 1.02 \times 10^{-12}S$
	$\Delta K_I \geq 12.04$	
		$n = 1.95$ $S = 2.5$ $C_0 = 1.01 \times 10^{-7}S$

Additionally, per A-4300(b)(2) of Reference [8.1], if the fatigue crack growth rate from light-water reactor environments is lower than air environments, the rate in air should be used.

[ ] Weld Metal

Flaw growth in the IDTB Weld ([ ]) and/or Alloy Nozzle in contact with air due to cyclic loading is calculated using the fatigue crack growth model presented in NUREG/CR-6907, Reference [8.6]. As per reference [8.6] a multiplier of 2 is applied to the Alloy 600 crack growth rate. Crack growth analysis is then conducted on a cycle-by-cycle basis to the end of service life. The crack growth rate equation for [ ] in air to be used is then given by:

$$\frac{da}{dN} = 2\,C\,S_R(\Delta K)^n$$

Where ΔK is the stress intensity factor range in terms of MPa√m and da/dN is the crack growth rate in terms of m/cycle, and

$C = 4.835\text{x}10^{-14} + 1.622\text{x}10^{-16}T - 1.490\text{x}10^{-18}T^2 + 4.355\text{x}10^{-21}T^3$
$S_R = [1 - 0.82R]^{-2.2}$
T = degrees C
$n = 4.1$
$R = K_{min} / K_{max}$

The fatigue growth rate of [ ] in contact with light-water reactor environment due to cyclic loading is calculated using the fatigue crack growth model presented in NUREG/CR-6907, Reference [8.6]. As per reference [8.6] a multiplier of 2 is applied to the Alloy 600 crack growth rate. Crack growth analysis is then conducted on a cycle-by-cycle basis to the end of service life. The crack growth rate equation for [ ] in light water environment to be used is then given by:

$$\frac{da}{dN} = 2\,C\,S_R S_{ENV}(\Delta K)^n$$

Where ΔK is the stress intensity factor range in terms of MPa√m and da/dN is the crack growth rate in terms of m/cycle, and

$C = 4.835\text{x}10^{-14} + 1.622\text{x}10^{-16}T - 1.490\text{x}10^{-18}T^2 + 4.355\text{x}10^{-21}T^3$

$S_R = [1 - 0.82R]^{-2.2}$
$S_{ENV} = 1 + A(C\ S_R\ \Delta K^n)^{m-1}\ T_R^{1-m}$
$A = 4.4 \times 10^{-7}$
$m = 0.33$
T = degrees C
$n = 4.1$
$R = K_{min} / K_{max}$
T_R = rise time, set at 30 seconds

2.4 Fatigue Crack Growth Calculations

For the flaw types postulated along paths 1a/b/c and 2a/b/c, the AREVACGC EXCEL based program, Reference [8.5], will be used to perform the fatigue crack growth calculation and estimate the final flaw size.

For the cylindrical flaws postulated along paths 3a/b/c and 4a/b/c, crack growths were estimated using EXCEL spread sheets. Crack growths for paths 3a/b/c and 4a/b/c are calculated by incrementally adding crack growth for one year at the time. Crack growth for one year is the summation of crack growth due to all transients for one year. Crack growth is incrementally linked such that the crack growth contribution from one transient is used to update the crack depth for the subsequent transient.

2.5 Acceptance Criteria

For postulated axial and circumferential flaws in the [ ] repair weld the acceptance criteria in IWB-3642, Reference [8.1] is used. IWB-3642 states that "piping containing flaws exceeding the acceptance standards of IWB-3514.1 may be evaluated using analytical procedures described in Appendix C and is acceptable for continued service during the evaluated time period when the critical flaw parameters satisfy the criteria in Appendix C." According to C-4230, Reference [8.1], for flaws in Ni-Cr-Fe weld metal, flaw evaluation procedures of C-4210 shall be used. Based on Figure C-4210-1 of Reference [8.1], for a flaw in austenitic/Ni-Cr-Fe weld material that uses non-flux welds, Section C-5000, Reference [8.1], is to be used for flaw evaluation.

For the postulated cylindrical flaw in the low alloy steel RVCH material, IWB-3612 acceptance criteria of Section XI, Reference [8.1] is used. According to IWB-3612 a flaw is acceptable if the applied stress intensity factor for the flaw dimension a_f satisfy the following criteria.

(a) For normal and upset conditions:

$K_I < K_{Ia} / \sqrt{10}$

Where:
K_I = applied stress intensity factor for normal, upset, and test conditions for flaw dimension a_f.
K_{Ia} = fracture toughness based on crack arrest for the corresponding crack-tip temperature
a_f = end-of-evaluation-period flaw depth

(b) For emergency, faulted, and test conditions:

$K_I < K_{Ic} / \sqrt{2}$

Where:
K_I = applied stress intensity factor for emergency, faulted, and test conditions for flaw dimension a_f.
K_{Ic} = fracture toughness based on crack initiation for the corresponding crack-tip temperature
a_f = end-of-evaluation-period flaw depth

For the postulated cylindrical flaw in the [ ] weld repair material, IWB-3612 acceptance criteria is not evaluated since a limit load solution is not available for such a flaw in the ASME B&PV Code, Reference [8.1]. The shear stress at the remaining ligament for the maximum crack growth for this flaw type at the end of the plant life is evaluated per NB-3227.2, Reference [8.10].

3.0 ASSUMPTIONS

3.1 Unverified Assumptions

There are no unverified assumptions used herein. Justified assumptions and modelling simplifications are detailed in the following sections.

3.2 Justified Assumptions

3.2.1 The anomaly is postulated to include a "crack-like" defect, located at the upper and lower "triple-point" locations. For analytical purposes, a continuous circumferential flaw is located in the horizontal plane. Another continuous flaw is located in the cylindrical plane between the weld and RVCH.

3.2.2 In the radial plane, the anomaly is assumed to include a quarter-circular "crack-like" defect. For analytical purposes, a semi-circular flaw is used to represent the radial cross-section of the anomaly.

3.2.3 In the interface of IDTB weld and RVCH bore, the anomaly is assumed to include a cylindrical-flaw like defect. For analytical purposes, a flaw in a semi-infinite plate is used to represent the radial cross-section of the anomaly.

3.2.4 The CRDM housing nozzles function as mechanical mounts for the CRDM. The CRDM are relatively tall, slender structures that may be subjected to seismic or other motions resulting in bending loads on the 'CRDM nozzle-to-head connection' weld. However, mechanical loads from the CRDM are transmitted to the head through the interference fit region. The design feature effectively shields the 'CRDM nozzle-to-head connection' weld from being subject to external loads. Therefore, external loads are not applicable to the CRDM nozzle weld repair. The same justified assumption applies to the RVLIS and CETC Nozzles. No external loads are considered on the existing nozzle which extends above the RVCH top surface.

3.3 Modelling Simplifications

3.3.1 Dimensions used for the analyses are based on nominal values. This is considered to be standard practice in stress analysis and fracture mechanics analysis.

4.0 DESIGN INPUTS

The regions of interest for the present flaw evaluations are the upper and lower triple point locations, where three different materials intersect. These materials are the existing or the replacement Nozzle material, the new IDTB repair weld material and the RVCH material. The Byron/Braidwood existing Nozzle is made of SB-167 Alloy 600 material, the replacement nozzle is made of SB-166 Alloy 690, the new weld is made of [ ], and the RVCH is fabricated of SA-533 Grade B Class 1, Reference [8.2].

4.1 Geometry

Pertinent geometry parameters used for flaw evaluations are provided below:

Paths 1a/b/c & 2a/b/c:

The following dimensions are used for evaluating the 360° circumferential flaw and axial flaw postulated along paths 1a/b/c & 2a/b/c. Dimensions obtained from Reference [8.7] bounds the dimensions from CRDM and RVLIS IDTB weld, Reference [8.12].

Existing Nozzle/Bore OD = [ ] in	Reference [8.7]
Existing Nozzle ID = [ ] in	Reference [8.7]
Path 1a/b/c Thickness, t_1 = [ ] in	
Replacement Nozzle OD = [ ] in	Reference [8.7] – See Note 20 and Diameter "D1"
Repair Nozzle ID at IDTB Weld = [ ] in	Reference [8.8]
Path 2a/b/c Thickness, t_2 = [ ] in	
Initial flaw depth, ai = 0.1 in	Reference [8.2]

Paths 3a/b/c & 4a/b/c:

The cylindrical flaws postulated along paths 3a/b/c and 4a/b/c propagate along the interface between the IDTB repair weld and the RV Closure Head. The controlling length of this interface is 1.28 inches at paths 3a/b/c and 4a/b/c, References [8.7] and [8.12]. The initial flaw depth is postulated to be 0.1 inches, Reference [8.2].

4.2 Material Strength

Reference [8.3] provides the material strength pertinent for the flaw evaluation assessment of the weld anomaly in this document. Table 4-1 lists the values of yield strength (σ_y) and ultimate strength (σ_{ult}).

Table 4-1 - Material Strength

Material	Component	Temp. (°F)	Yield Strength, σ_y (ksi)	Ultimate Strength, σ_{ult} (ksi)
SA-533 Gr. B Cl. 1	RVCH	[		]
Weld Filler [ ] Equivalent SB-166 Alloy 690 properties	IDTB Weld			

Note (1): Interpolated values.

4.3 Fracture Toughness

4.3.1 Low Alloy Steel RV Head Material

The maximum nil ductility temperature (RT_{NDT}) for the low alloy steel RVCH is [ ] for Byron Unit 1, Reference [8.11]. Fracture toughness curves for SA-533 Grade B Class 1 material is illustrated in Figure A-4200-1 of Reference [8.1]. At an operating temperature of about [ ] Reference [8.3], the K_{Ia} fracture toughness values for this material is (using RT_{NDT} of [ ]) are above 200 ksi√in. An upper bound value of 200 ksi√in will be conservatively used for the present flaw evaluations.

4.3.2 [ ] Material

Brittle fracture is not a credible failure mechanism for ductile materials such as [ ] the failure mechanism for the [ ] materials is limit load or ductile crack extension (EPFM). IWB-3612 acceptance criteria for the cylindrical flaw postulated in the repair weld are not evaluated since a limit load solution is not available for such a flaw in the ASME B&PV Code, Reference [8.1]. The shear stress at the remaining ligament for the maximum crack growth in the [ ] weld repair material at the end of the plant life is evaluated per NB-3227.2, Reference [8.10].

4.4 Applied Stresses Intensity Factor Calculation

As mentioned in Section 2.2, the weight function method implemented in AREVACGC, Reference [8.5] was used to calculate the SIF for the OD continuous circumferential and axial surface flaws. For the cylindrical flaw, the SIF solution given in Appendix A of the 2001 Edition of Section XI, Reference [8.1] was used to calculate the SIF solution.

4.4.1 Transient Stresses

The cyclic operating stresses that are needed to calculate fatigue crack growth are obtained from a thermo-elastic finite element analysis, Reference [8.3]. These cyclic stresses are developed for all the transients at a number of time points to capture the maximum and minimum stresses due to fluctuations in pressure and temperature. Per References [8.3], the number of RCS design transients is established for 40 years of design life. Cyclic operating stresses were generated in Reference [8.3] for the transients listed in Reference [8.4]. The transients that have trivial contribution to fatigue are not considered per Reference [8.3]. The transient cycle counts used in this calculation are obtained from Reference [8.4]. The operating transients are listed in Table 4-2.

All radial paths go from ID to OD of the IDTB weld; all the vertical paths go from bottom to top. Stresses are provided for 12 equidistant intervals along the path lines.

Table 4-2 – Operating Transients and Cycles

Condition	Transient	File Name Convention	Number of Cycles
Normal			
Upset			
Emergency			
Faulted			
Test			
Upset			

[ ]

4.4.2 External Loads

The CRDM housing nozzles function as mechanical mounts for the CRDM. The CRDM are relatively tall, slender structures that may be subjected to seismic or other motions resulting in bending loads on the 'CRDM nozzle-to-head connection' weld. However, mechanical loads from the CRDM are transmitted to the head through the interference fit region. The design feature effectively shields the 'CRDM nozzle-to-head connection' weld from being subject to external loads. Therefore, external loads are not applicable to the CRDM nozzle weld repair. The same justified assumption applies to the RVLIS and CETC Nozzles. No external loads are considered on the existing nozzle which extends above the RVCH top surface.

4.4.3 Replacement Nozzle Loads

Loads at the existing J-groove weld due to loads on the nozzle inside the vessel are supplied in PWROG-14067, Reference [8.4] and shown in Table 4-3. These will be referred to as 'Internal' loads to avoid confusion with loads occurring outside the vessel. The new repair nozzle is secured by the IDTB weld. Therefore, these same loads will be used to determine the stress distribution acting on the path lines due to loading from inside the vessel. [ ] cycles of OBE seismic loading, per TODI-BYR-15-012, Reference [8.4], will be considered.

Table 4-3 – Replacement Nozzle Internal Mechanical Loads

Load Description	Axial (lbs)	Shear (lbs)	Bending Moment (in-lbs)
Deadweight			
Flow-Induced Vibration + Pump-Induced Vibration			
OBE			

The effect of deadweight and flow/pump induced vibration loads is addressed by adding these loads as additional stresses to the transient and residual stresses for fatigue crack growth evaluation in AREVACGC, Reference [8.5]. Seismic effects are addressed as described in Section 4.4.4.

4.4.4 Seismic Event

The effect of the seismic OBE loads on fatigue crack growth is addressed by modeling the seismic event as a transient event. The OBE loads as obtained from Reference [8.4] acting on the path lines are shown in Table 4-3. These OBE loads are converted to axial stresses according to

$$Axial\ Stress = \frac{F_{axial}}{A} + \frac{M_{bending}}{S_o}$$

Where S_o is the OD section modulus conservatively used in the calculation. The results are given in Table 4-4.

Table 4-4 – Axial Stresses due to Seismic Loads

OBE (+/-)	Path Line	
	1a/1b/1c	2a/2b/2c
Axial Stress, psi	[ ]	[ ]

The baseline through-wall axial stress distribution for each path line is obtained from the stress state at the steady state conditions. This corresponds to the last time point of transient HU. Per TODI-BYR-15-012, Reference [8.4], the total lifetime number of OBE cycles is [ ]

4.4.5 Residual Stresses

A three-dimensional elastic-plastic finite element analysis, Reference [8.9] was performed to simulate the sequence of steps involved in arriving at the configuration of the weld repair of CRDM/RVLIS/CETC Nozzle in the RVCH of Byron/Braidwood Units 1 and 2. The residual stress analysis, Reference [8.9], simulated welding of the existing J-groove weld and butter; machining of the nozzle and IDTB weld prep; attaching Alloy 690 replacement nozzle; welding of the IDTB weld repair with [ ] Operation at steady state temperature and pressure conditions and return to zero load conditions was also simulated after the completion of the weld simulation.

The residual stresses are provided by Reference [8.9] for the path lines identified in Figure 2-1. All radial paths go from OD to ID of the IDTB weld; all the vertical paths go from top to bottom. Stresses are provided for 20 equidistant intervals along the path lines. Since transient stresses provided in Reference [8.3] are provided for 12 equidistant intervals along the path lines, residual stresses are mapped to 12 equidistant intervals and to go from ID to OD of the IDTB weld (radial paths) and from bottom to top (vertical paths) to match stress distribution from Reference [8.3]. Weld residual stresses are linearly added to the transient stresses.

5.0 CALCULATIONS

Assessment of a flaw like triple point anomaly in the Byron/Braidwood Nozzle repair was completed using three flaw types that were postulated to form in the vicinity of the triple point. For every postulated flaw type a crack growth analysis was conducted to determine the final flaw size after 40 years of operation. After the final flaw size is determined, the flaw is assessed to determine the safety margins and compliance with the flaw acceptance criteria outlined in Section 2.5.

5.1 Circumferential Flaw for Paths 1a/b/c & 2a/b/c

5.1.1 Circumferential Flaw Growth Analysis (Paths 1a/b/c and 2a/b/c)

AREVACGC, Reference [8.5] was used to determine the final flaw depth due to fatigue crack growth. A summary of the final flaw depths is given in Table 5-1 for paths 1a, 1b, 1c, 2a, 2b and 2c. Contribution of the individual transients to crack growth is given in Table 5-2 for paths 1a, 1b, 2a, and 2b and in Table 5-3 for paths 1c and 2c.

Table 5-1 – Crack Growth for 360° Circumferential Flaw (Paths 1a/b/c and 2a/b/c)

Path	Path 1a	Path 1b	Path 1c	Path 2a	Path 2b	Path 2c
Initial Flaw Depth (in) =	0.1000	0.1000	0.1000	0.1000	0.1000	0.1000
Initial a/t ratio =						
Final Flaw Depth (in) =						
Final a/t ratio =						
Total amount of Fatigue Crack Growth (in) =						

Table 5-2 – Individual Transient Contribution to Crack Growth for 360° Circumferential Flaw (Paths 1a/b and 2a/b)

Path	Path 1a		Path 1b		Path 2a		Path 2b	
Transient	Growth (in)	Percent	Growth (in)	Percent	Growth (in)	Percent	Growth (in)	Percent

Table 5-3 – Individual Transient Contribution to Crack Growth for 360° Circumferential Flaw (Paths 1c and 2c)

Path	Path 1c		Path 2c	
Transient	Growth (in)	Percent	Growth (in)	Percent

5.1.2 Flaw Evaluation for OD Circumferential Flaw (Paths 1a/b/c & 2a/b/c)

As mentioned in Section 2.5, Article C-5000 of Reference [8.1] contains the appropriate flaw evaluation procedure for the end of life OD circumferential flaw. As shown in Table 5-1, since the final flaw depth along path 2a is the greatest between the other paths, the final flaw depth for path 2a is used for the end of life flaw evaluation and conservatively using the dimensions of paths 1a/b/c which have the smallest thicknesses. Table 5-4 shows details of the end of life flaw evaluation analysis performed to assess the postulated continuous circumferential flaw. It is seen from Table 5-4 that the allowable stress is higher than the applied membrane stress by 3.38 times safety factor.

Table 5-4 – End of Life Evaluation for Continuous External Circumferential Flaw (Limit Load)

Yield Strength, σ_y =	[ ]	ksi
Ultimate Strength, σ_{ult} =	[ ]	ksi
Pressure, p =	[ ]	psi
Outside Radius, R_o =	[ ]	in
Inside Radius, R_i =	[ ]	in
Mean Radius, R_m =	[ ]	in
Thickness, t =	[ ]	in
Final Flaw Depth, a_f =	[ ]	in
$\sigma_m = pD_o/4t$ =	[ ]	ksi
Flow strength, σ_f =	[ ]	ksi
Safety Factor, SF_m =	2.7	
θ =	3.1416	rad
$\sigma_m^c = \sigma_f / [1-(a/t)(\theta/\pi)-2\phi/\pi]$ =	[ ]	ksi
$\phi = \arcsin[0.5(a/t)\sin\theta]$ =	0	rad
$S_t = \sigma_m^c / SF_m$ =	[ ]	ksi
Margin, S_t/σ_m =	[ ]	

5.2 Axial Flaw for Paths 1a/b/c & 2a/b/c

5.2.1 Axial Flaw Growth Analysis (Paths 1a/b/c & 2a/b/c)

AREVACGC, Reference [8.5] was used to determine the final flaw depth due to fatigue crack growth. For each path (1a/b/c & 2a/b/c) crack growth was performed using depth location (radial) and surface location (axial) SIF. A summary of the final radial and axial flaw depths is given in Table 5-5 and Table 5-6, respectively, for paths 1a, 1b, 1c, 2a, 2b, and 2c. Contribution of the individual transients to radial and axial crack growth is given in Table 5-7 and Table 5-8, respectively for paths 1a, 1b, 2a, and 2b and in Table 5-9 and Table 5-10 for paths 1c and 2c.

Table 5-5 – Radial Crack Growth for Axial Flaw

Path	Path 1a	Path 1b	Path 1c	Path 2a	Path 2b	Path 2c
Initial Flaw Depth (in) =	0.1000	0.1000	0.1000	0.1000	0.1000	0.1000
Initial a/t ratio =	[					]
Final Flaw Depth (in) =						
Final a/t ratio =						
Total amount of Fatigue Crack Growth (in) =						

Table 5-6 – Axial Crack Growth for Axial Flaw

Path	Path 1a	Path 1b	Path 1c	Path 2a	Path 2b	Path 2c
Initial Flaw Depth (in) =	0.1000	0.1000	0.1000	0.1000	0.1000	0.1000
Initial a/t ratio =	[					]
Final Flaw Depth (in) =						
Final a/t ratio =						
Total amount of Fatigue Crack Growth (in) =						

Table 5-7 – Individual Transient Contribution to Radial Crack Growth for Axial Flaw (Paths 1a/b and 2a/b)

Path	Path 1a		Path 1b		Path 2a		Path 2b	
Transient	Growth (in)	Percent	Growth (in)	Percent	Growth (in)	Percent	Growth (in)	Percent

Table 5-8 – Individual Transient Contribution to Axial Crack Growth for Axial Flaw (Paths 1a/b and 2a/b)

Path	Path 1a		Path 1b		Path 2a		Path 2b	
Transient	Growth (in)	Percent	Growth (in)	Percent	Growth (in)	Percent	Growth (in)	Percent

Table 5-9 – Individual Transient Contribution to Radial Crack Growth for Axial Flaw (Paths 1c and 2c)

Path	Path 1c		Path 2c	
Transient	Growth (in)	Percent	Growth (in)	Percent

Table 5-10 – Individual Transient Contribution to Axial Crack Growth for Axial Flaw (Paths 1c and 2c)

Path	Path 1c		Path 2c	
Transient	Growth (in)	Percent	Growth (in)	Percent

5.2.2 Flaw Evaluation for OD Axial Flaw (Paths 1a/b/c & 2a/b/c)

As mentioned in Section 2.5, Article C-5000 of Reference [8.1] contains the appropriate flaw evaluation procedure for the end of life OD axial flaw. As shown in Table 5-5 and Table 5-6 the maximum flaw depth is [ ] for a flaw along path 2a considering an axial crack growth of [ ] This flaw depth was used for the end of life flaw evaluation of the postulated OD axial flaw. Table 5-11 shows details of the end of life flaw evaluation of the postulated OD axial flaw. It is shown in Table 5-11, that both the final flaw depth and length, after 40 years of crack growth, are less than the allowable flaw depth and length.

Table 5-11 – End of Life Evaluation for External Axial Flaw (Limit Load)

Yield Strength, σ_y =	[ ]	ksi
Ultimate Strength, σ_{ult} =	[ ]	ksi
Flow strength, σ_f =	[ ]	ksi
Pressure, p =	[ ]	psi
Outside Radius, R_o =	[ ]	in
Inside Radius, R_i =	[ ]	in
Mean Radius, R_m =	[ ]	in
Thickness, t =	[ ]	in
Final Flaw Depth, a_f =	[ ]	in
Final Flaw Length, $l_f = 2 \times a_f$ =	[ ]	in
$\sigma_h = pR_m/t$ =	[ ]	ksi
$l_{allow} = 1.58(R_m t)^{0.5} [(\sigma_f/\sigma_h)^2 - 1]^{0.5}$ =	[ ]	in^2
$M_2 = [1 + (1.61 / 4R_m t) l_f^2)]^{0.5}$	[ ]	
Safety Factor, SF_m =	2.7	
Stress Ratio = $SF_m\ \sigma_h/\sigma_f$ =	[ ]	
Nondimensional Flaw Length, $l_f/\sqrt{R_m t}$ =	[ ]	
Allowable a/t	[ ]	Table C-5410-1, Reference [8.1]
Allowable Flaw Depth, a_{allow} =	[ ]	
Margin, a_{allow} / a_f =	[ ]	

5.3 Cylindrical Flaw for Paths 3a/b/c & 4a/b/c

5.3.1 Cylindrical Flaw Growth Analysis (Paths 3a/b/c & 4a/b/c)

For the cylindrical flaws, crack growth was calculated in accordance with Section 2.4. Crack growth for first year is shown in Table 5-12 through Table 5-23 for paths 3a, 3b, 3c, 4a, 4b, and 4c, respectively. Final crack depths for the cylindrical flaws for all paths are shown in Table 5-24 and Table 5-25.

Table 5-12 – First Year Crack Growth for Cylindrical Flaw along Path 3a (Bottom Corner)

Transient	K_{max} (ksi√in)	K_{min} (ksi√in)	ΔK (ksi√in)	ΔN (cycle/year)	$\Delta a = \Delta N\ C_0(\Delta K)^n$ (in)

Table 5-13 – First Year Crack Growth for Cylindrical Flaw along Path 3b (Bottom Corner)

Transient	K_{max} (ksi√in)	K_{min} (ksi√in)	ΔK (ksi√in)	ΔN (cycle/year)	$\Delta a = \Delta N\ C_0(\Delta K)^n$ (in)

Table 5-14 – First Year Crack Growth for Cylindrical Flaw along Path 3c (Bottom Corner)

Transient	K_{max} (ksi√in)	K_{min} (ksi√in)	ΔK (ksi√in)	ΔN (cycle/year)	$\Delta a = \Delta N\ C_0(\Delta K)^n$ (in)

Table 5-15 – First Year Crack Growth for Cylindrical Flaw along Path 4a (Bottom Corner)

Transient	K_{max} (ksi√in)	K_{min} (ksi√in)	ΔK (ksi√in)	ΔN (cycle/year)	$\Delta a = \Delta N\ C_0(\Delta K)^n$ (in)

Table 5-16 – First Year Crack Growth for Cylindrical Flaw along Path 4b (Bottom Corner)

Transient	K_{max} (ksi√in)	K_{min} (ksi√in)	ΔK (ksi√in)	ΔN (cycle/year)	$\Delta a = \Delta N\ C_0(\Delta K)^n$ (in)

Table 5-17 – First Year Crack Growth for Cylindrical Flaw along Path 4c (Bottom Corner)

Transient	K_{max} (ksi√in)	K_{min} (ksi√in)	ΔK (ksi√in)	ΔN (cycle/year)	$\Delta a = \Delta N\ C_o(\Delta K)^n$ (in)

Table 5-18 – First Year Crack Growth for Cylindrical Flaw along Path 3a (Top Corner)

Transient	K_{max} (ksi√in)	K_{min} (ksi√in)	ΔK (ksi√in)	ΔN (cycle/year)	$\Delta a = \Delta N\ C_0(\Delta K)^n$ (in)

Table 5-19 – First Year Crack Growth for Cylindrical Flaw along Path 3b (Top Corner)

Transient	K_{max} (ksi√in)	K_{min} (ksi√in)	ΔK (ksi√in)	ΔN (cycle/year)	$\Delta a = \Delta N\ C_0(\Delta K)^n$ (in)

Table 5-20 – First Year Crack Growth for Cylindrical Flaw along Path 3c (Top Corner)

Transient	K_{max} (ksi√in)	K_{min} (ksi√in)	ΔK (ksi√in)	ΔN (cycle/year)	$\Delta a = \Delta N\ C_0(\Delta K)^n$ (in)

Table 5-21 – First Year Crack Growth for Cylindrical Flaw along Path 4a (Top Corner)

Transient	K_{max} (ksi√in)	K_{min} (ksi√in)	ΔK (ksi√in)	ΔN (cycle/year)	$\Delta a = \Delta N\ C_0(\Delta K)^n$ (in)

Table 5-22 – First Year Crack Growth for Cylindrical Flaw along Path 4b (Top Corner)

Transient	K_{max} (ksi√in)	K_{min} (ksi√in)	ΔK (ksi√in)	ΔN (cycle/year)	$\Delta a = \Delta N\ C_o(\Delta K)^n$ (in)

Table 5-23 – First Year Crack Growth for Cylindrical Flaw along Path 4c (Top Corner)

Transient	K_{max} (ksi√in)	K_{min} (ksi√in)	ΔK (ksi√in)	ΔN (cycle/year)	$\Delta a = \Delta N\ C_0(\Delta K)^n$ (in)

Table 5-24 – Final Crack Depth for Cylindrical Flaw (Bottom Corner)

Path	Crack Depth (in)
Path 3a	[ ]
Path 3b	[ ]
Path 3c	[ ]
Path 4a	[ ]
Path 4b	[ ]
Path 4c	[ ]

Table 5-25 – Final Crack Depth for Cylindrical Flaw (Top Corner)

Path	Crack Depth (in)
Path 3a	[ ]
Path 3b	[ ]
Path 3c	[ ]
Path 4a	[ ]
Path 4b	[ ]
Path 4c	[ ]

5.3.2 Fracture Toughness Margin for Cylindrical Flaw (Paths 3a/b/c & 4a/b/c)

As mentioned in Section 2.5, for the postulated cylindrical flaw in the low alloy steel RV closure head material, IWB-3612 acceptance criteria of Section XI, Reference [8.1] is used. According to IWB-3612, a flaw is acceptable if the applied stress intensity factor for the flaw dimension a_f satisfy the criteria that $K_I < K_{Ia}/\sqrt{10}$ for normal/upset conditions and $K_I < K_{Ic}/\sqrt{2}$ for emergency/faulted/test conditions.

To determine the fracture toughness margin, the maximum applied stress intensity factor for all time points is determined for each flaw path. The effective stress intensity factor is then determined based on the theory in Reference [8.1]. The temperature (T) is the minimum (limiting) temperature of each transient. The minimum temperatures of most limiting transients are shown along with corresponding K_{Ia}'s are shown in Table 5-26. In Table 5-26, it is shown that the calculated minimum LEFM margins are [ ] for service level A and B and [ ] for Emergency/Faulted/Test Conditions, and are thus higher than the required margin of $\sqrt{10}$ (Level A & B) and $\sqrt{2}$ (Level C & D), respectively.

For the postulated cylindrical flaws in the [ ] weld repair material, IWB-3612 acceptance criteria is not evaluated since a limit load solution is not available for such a flaw in the ASME B&PV Code, Reference [8.1]. The shear stress at the remaining ligament for the maximum crack growth for this flaw type at the end of the plant life is evaluated below per NB-3227.2, Reference [8.10].

Table 5-26 – LEFM Margin for Cylindrical Flaw

	Path & Location	Limiting Transients	a_f (in)	K_{Ieff} (ksi√in)	Temp. (°F)	K_{Ia} (ksi√in)	Margin K_{Ia} / K_{Ieff}	
Levels A/ B	Path 4a (Head Bottom)	[					]	> 3.16
	Path 4b (Head Bottom)							
	Path 4c (Head Bottom)							
	Path 4a (Head Top)							
	Path 4b (Head Top)							
	Path 4c (Head Top)							
						K_{IC} (ksi√in)	Margin K_{Ia} / K_{Ieff}	
Levels C/ D/ Test	Path 4a (Head Bottom)	[					]	> 1.41
	Path 4b (Head Bottom)							
	Path 4c (Head Bottom)							
	Path 4a (Head Top)							
	Path 4b (Head Top)							
	Path 4c (Head Top)							

Notes (1): $K_{Ieff} < 0$ and therefore there is no crack growth for service level.

The shear stress at the remaining ligament is also calculated as follows:

$\tau = (P_{axial_H} + P_{axial_Internal})/(A_s)$

Where:

$P_{axial_H} = (\pi/4) \times P \times D_o^2 = (\pi/4)$ [ ] Reference [8.3]

$P_{axial_Internal} =$ [ ] Table 4-3

$A_s = 2 \times \pi \times [L_{final} \times D_o/2]$

Where L_{final} is the remaining ligament of the IDTB weld/head interface after crack growth at paths 3a, 3b, 3c, 4a, 4b, and 4c. The maximum crack growth among cracks along paths 3a, 3b, 3c, 4a, 4b, and 4c is for path 4b at the bottom corner and the final flaw size is [ ] (Table 5-24). Thus the area of the remaining ligament is found as

$A_s =$ [ ]

Thus the shear stress, $\tau = (P_{axial_H} + P_{axial_Internal})/(A_s) =$ [ ]

Per NB-3227.2, Reference [8.10], the maximum allowable average primary shear stress in IDTB weld is $0.6S_m$, which equals 13.98 ksi (with Sm equal to 23.3 ksi, Reference [8.3]). Therefore the remaining ligament of the IDTB weld has a lower shear stress than allowable shear stress.

6.0 RESULTS

The flaw evaluation results for 40 years of fatigue crack growth are as follows.

6.1 Fatigue Crack Growth of Continuous External Circumferential Flaw

a) Fatigue crack growth analysis:

Initial flaw size, $a_i = 0.1000$ in.

Final flaw size, $a_f =$ [ ]

b) End of Life (Limit load) analysis:

Margin, [ ]

6.2 Fatigue Crack Growth of Semi-Circular External Axial Flaw

a) Fatigue crack growth analysis:

Initial flaw size, $a_i = 0.1000$ in.

Final flaw size, $a_f =$ [ ]

b) End of Life (Limit load) analysis:

Margin, [ ]

6.3 Fatigue Crack Growth of Continuous Cylindrical Flaw along Paths 3a & 4a

RVCH (Path 4a Bottom Tip)

Initial flaw size, $a_i = 0.1000$ in.

Final flaw size, $a_f =$ [ ]

Level A and B Stress intensity factor at final flaw size, $K_{Ieff} =$ [ ]

Level A and B Fracture toughness, $K_{Ia} =$ [ ]

Level A and B Fracture toughness margin, $K_{Ia} / K_{Ieff} =$ [ ] $> \sqrt{10}$

Level C, D, and Test Stress intensity factor at final flaw size, $K_{Ieff} =$ [ ]

Level C, D, and Test Fracture toughness, $K_{IC} =$ [ ]

Level C, D, and Test Fracture toughness margin, $K_{IC} / K_{Ieff} =$ [ ] $> \sqrt{2}$

RVCH (Path 4a Top Tip)

Initial flaw size, $a_i = 0.1000$ in.

Final flaw size, $a_f =$ [ ]

Level A and B Stress intensity factor at final flaw size, $K_{Ieff} =$ [ ]

Level A and B Fracture toughness, $K_{Ia} =$ [ ]

Level A and B Fracture toughness margin, $K_{Ia} / K_{Ieff} =$ [ ] $> \sqrt{10}$

Level C, D, and Test Stress intensity factor at final flaw size, $K_{Ieff} =$ [ ]

Level C, D, and Test Fracture toughness, $K_{IC} =$ [ ]

Level C, D, and Test Fracture toughness margin, $K_{IC} / K_{Ieff} =$ [ ] $> \sqrt{2}$

Nozzle/IDTB Weld (Path 3a Bottom Tip)

Initial flaw size, $a_i = 0.1000$ in.

Final flaw size, $a_f =$ [ ]

Max. Shear Stress, $\tau =$ [ ] $< 0.6S_m = 13.98$ ksi

Nozzle/IDTB Weld (Path 3a Top Tip)

Initial flaw size, $a_i = 0.1000$ in.

Final flaw size, $a_f =$ [ ]

Max. Shear Stress, $\tau =$ [ ] $< 0.6S_m = 13.98$ ksi

6.4 Fatigue Crack Growth of Continuous Cylindrical Flaw along Paths 3b & 4b

RVCH (Path 4b Bottom Tip)

Initial flaw size, $a_i = 0.1000$ in.

Final flaw size, $a_f =$ [ ]

Level A and B Stress intensity factor at final flaw size, $K_{Ieff} =$ [ ]

Level A and B Fracture toughness, $K_{Ia} =$ [ ]

Level A and B Fracture toughness margin, $K_{Ia} / K_{Ieff} =$ [ ] $> \sqrt{10}$

Level C, D, and Test Stress intensity factor at final flaw size, $K_{Ieff} =$ [ ]

Level C, D, and Test Fracture toughness, $K_{IC} =$ [ ]

Level C, D, and Test Fracture toughness margin, $K_{IC} / K_{Ieff} =$ [ ] $> \sqrt{2}$

RVCH (Path 4b Top Tip)

Initial flaw size, $a_i = 0.1000$ in.

Final flaw size, $a_f =$ [ ]

Level A and B Stress intensity factor at final flaw size, $K_{Ieff} =$ [ ]

Level A and B Fracture toughness, $K_{Ia} =$ [ ]

Level A and B Fracture toughness margin, $K_{Ia} / K_{Ieff} =$ [ ]

Level C, D, and Test Stress intensity factor at final flaw size, $K_{Ieff} =$ [ ]

Level C, D, and Test Fracture toughness, $K_{IC} =$ [ ]

Level C, D, and Test Fracture toughness margin, $K_{IC} / K_{Ieff} =$ [ ]

Nozzle/IDTB Weld (Path 3b Bottom Tip)

Initial flaw size, $a_i = 0.1000$ in.

Final flaw size, $a_f =$ [ ]

Max. Shear Stress, $\tau =$ [ ] ksi $< 0.6S_m = 13.98$ ksi

Nozzle/IDTB Weld (Path 3b Top Tip)

Initial flaw size, $a_i = 0.1000$ in.

Final flaw size, $a_f =$ [ ]

Max. Shear Stress, $\tau =$ [ ] $< 0.6S_m = 13.98$ ksi

6.5 Fatigue Crack Growth of Continuous Cylindrical Flaw along Paths 3c & 4c

RVCH (Path 4c Bottom Tip)

Initial flaw size,	$a_i = 0.1000$ in.
Final flaw size,	$a_f =$ [ ]
Level A and B Stress intensity factor at final flaw size,	$K_{Ieff} =$ [ ]
Level A and B Fracture toughness,	$K_{Ia} =$ [ ]
Level A and B Fracture toughness margin,	$K_{Ia} / K_{Ieff} =$ [ ] $> \sqrt{10}$
Level C, D, and Test Stress intensity factor at final flaw size,	$K_{Ieff} =$ [ ]
Level C, D, and Test Fracture toughness,	$K_{IC} =$ [ ]
Level C, D, and Test Fracture toughness margin,	$K_{IC} / K_{Ieff} =$ [ ] $> \sqrt{2}$

RVCH (Path 4c Top Tip)

Initial flaw size,	$a_i = 0.1000$ in.
Final flaw size,	$a_f =$ [ ]
Level A and B Stress intensity factor at final flaw size,	$K_{Ieff} =$ [ ]
Level A and B Fracture toughness,	$K_{Ia} =$ [ ]
Level A and B Fracture toughness margin,	$K_{Ia} / K_{Ieff} =$ [ ] $> \sqrt{10}$
Level C, D, and Test Stress intensity factor at final flaw size,	$K_{Ieff} =$ [ ]
Level C, D, and Test Fracture toughness,	$K_{IC} =$ [ ]
Level C, D, and Test Fracture toughness margin,	$K_{IC} / K_{Ieff} =$ [ ] $> \sqrt{2}$

Nozzle/IDTB Weld (Path 3c Bottom Tip)

Initial flaw size,	$a_i = 0.1000$ in.
Final flaw size,	$a_f =$ [ ]
Max. Shear Stress,	$\tau =$ [ ] ksi $< 0.6S_m = 13.98$ ksi

Nozzle/IDTB Weld (Path 3c Top Tip)

Initial flaw size,	$a_i = 0.1000$ in.
Final flaw size,	$a_f =$ [ ]
Max. Shear Stress,	$\tau =$ [ ] ksi $< 0.6S_m = 13.98$ ksi

The results of the analysis demonstrate that a 0.10 inch weld anomaly is acceptable for a 40 year design life of the Byron/Braidwood RVCH CRDM/RVLIS/CETC Nozzle IDTB weld repair. The minimum fracture toughness margins for flaw propagation Paths 3a, 3b, 3c, 4a, 4b, and 4c have been shown to be acceptable as compared to the required margins of $\sqrt{10}$ for normal/upset conditions and $\sqrt{2}$ for emergency/faulted/test conditions per Section XI, IWB-3612 (Reference [8.1]). A limit load analysis was performed considering the ductile weld repair material along flaw propagation Paths 1a/b/c and 2a/b/c. The analysis showed that for the postulated circumferential flaw the minimum margin on allowable stress is [ ] For the axial flaw the minimum margin on allowable flaw depth is [ ] Fracture toughness margins have been demonstrated for the postulated cylindrical flaws at the RVCH. Also for cylindrical flaws at the RVCH and the IDTB weld it is shown that the applied shear stress at the remaining ligament is less than the allowable shear stress per NB-3227.2, Reference [8.10].

7.0 COMPUTER USAGE

7.1 Validation

To validate the installation of AREVACGC 5.0, Reference [8.5], Test Case 1 provided in Reference [8.5] (contained in TestCase1.xls) was executed. The installation of the software on a PC workstation is documented below and verification tests of similar applications are listed as follows.

- **Computer programs tested:** AREVACGC 5.0
- **Computer hardware used:** The hardware platform is Intel (R) Core(TM) i7-3520M CPU at 2.90 GHz, 8GB RAM and the Operating System is Microsoft Windows 7, version 2009, Service Pack 1, Serial Number CRPMYW1.
- **Name of person running the tests:** Luziana Reno
- **Date of tests:** 03/24/2015.
- **Acceptability:** Results agree with those documented for the corresponding test case in Reference [8.5].

7.2 Computer Files

Microsoft® Office Excel, along with the Excel macro program AREVACGC version 5.0, is used in the crack growth and SIF calculation. All computer analyses were run on Microsoft Windows 7, version 2009, Service Pack 1. The hardware is Intel (R) Core(TM) i7-3520M CPU at 2.90 GHz, 8GB RAM.

Computer files for all analysis contained in this document are listed in Table 7-1. These files have been stored in COLDSTOR server within the directory "\cold\General-Access\32\32-9000000\32-9237284-000\official."

Table 7-1 – Computer Files for Crack Growth Evaluation

File Name	Data and Time	Size (bytes)	Checksum	Description
BB12_Axial_SY(Hoop).xlsm	6/15/2015 09:07	1000598	57536	Axial flaw evaluation with AREVACGC for paths 1a/b and 2a/b
BB12_Axial_SY(Hoop)_90Deg.xlsm	6/15/2015 08:55	650584	17809	Axial flaw evaluation with AREVACGC for paths 1c and 2c
BB12_Circ_SZ(axial).xlsm	6/15/2015 08:33	805669	16224	Circumferential flaw evaluation with AREVACGC for paths 1a/b and 2a/b
BB12_Circ_SZ(axial)_90Deg.xlsm	6/15/2015 08:41	510418	42160	Circumferential flaw evaluation with AREVACGC for paths 1c and 2c
BB12_Edge_P3a_bot.xls	6/15/2015 08:17	1970176	11615	Cylindrical Flaw Evaluation Path 3a at Bottom Crack Tip
BB12_Edge_P3a_top.xls	4/9/2015 9:57	2,508,800	52764	Cylindrical Flaw Evaluation Path 3a at Top Crack Tip
BB12_Edge_P3b_bot.xls	6/15/2015 08:17	1912320	38861	Cylindrical Flaw Evaluation Path 3b at Bottom Crack Tip
BB12_Edge_P3b_top.xls	4/9/2015 9:57	2,445,312	17424	Cylindrical Flaw Evaluation Path 3b at Top Crack Tip
BB12_Edge_P3c_bot.xls	6/15/2015 08:17	1536000	25204	Cylindrical Flaw Evaluation Path 3c at Bottom Crack Tip
BB12_Edge_P3c_top.xls	4/9/2015 9:58	1,601,536	21300	Cylindrical Flaw Evaluation Path 3c at Top Crack Tip
BB12_Edge_P4a_bot.xls	6/15/2015 08:17	2074624	00047	Cylindrical Flaw Evaluation Path 4a at Bottom Crack Tip
BB12_Edge_P4a_top.xls	4/1/2015 15:45	2,436,608	05932	Cylindrical Flaw Evaluation Path 4a at Top Crack Tip
BB12_Edge_P4b_bot.xls	6/15/2015 08:12	2070528	03304	Cylindrical Flaw Evaluation Path 4b at Bottom Crack Tip
BB12_Edge_P4b_top.xls	4/1/2015 15:48	2,493,952	29849	Cylindrical Flaw Evaluation Path 4b at Top Crack Tip
BB12_Edge_P4c_bot.xls	6/15/2015 08:17	1541632	33030	Cylindrical Flaw Evaluation Path 4c at Bottom Crack Tip
BB12_Edge_P4c_top.xls	4/1/2015 15:49	1,608,192	34263	Cylindrical Flaw Evaluation Path 4c at Top Crack Tip
K1_edge_Verification.xls	4/2/2015 10:03	413,184	51845	Verification of KIeff_edge function
TestCase1.xls	3/24/2015 10:19	628,736	64581	Test case for verifying that AREVCGC 5.0 executes properly
TestCase1 - 6-15-2015.xls	6/15/2015 09:10	628736	40837	Test case for verifying that AREVCGC 5.0 executes properly after all runs were completed

8.0 REFERENCES

8.1 ASME Boiler and Pressure Vessel Code, Section XI, "Rules for Inservice Inspection of Nuclear Power Plant Components", 2001 Edition with 2003 Addenda.

8.2 AREVA Document 08-9232121-000, Specification, "Byron Units 1 and 2, and Braidwood Units 1 and 2, RVCH Nozzle and Penetration Modification"

8.3 AREVA Document 32-9233803-000, "ASME Section III Analysis of Byron/Braidwood RVCH Nozzle and Penetration Modification"

8.4 AREVA Document 38-2201373-000, "Byron Units 1 and 2 and Braidwood Units 1 and 2 Proprietary Information"

8.5 AREVA Document 32-9055891-006, "Fatigue and PWSCC Crack Growth Evaluation Tool AREVACGC" (Proprietary Document)

8.6 NUREG/CR-6907, "Crack Growth Rates of Nickel Alloy Welds in a PWR Environment", U.S. Nuclear Regulatory Commission (Argonne National Laboratory), May 2006

8.7 AREVA Drawing 02-9232824E-000, "Byron Units 1 and 2/Braidwood Units 1 and 2 Thermocouple Column Penetration Modification"

8.8 AREVA Drawing 02-9232827D-000, "Byron Units 1 and 2/Braidwood Units 1 and 2 Replacement Thermocouple Housing Extension"

8.9 AREVA Document 32-9233779-000, "Weld Residual Stress Analysis of Byron 1 & 2, and Braidwood 1 & 2 RVCH Nozzle/Penetration Repair"

8.10 ASME Boiler and Pressure Vessel Code, Section III, "Nuclear Facility Components", Division 1, 2001 Edition with 2003 Addenda.

8.11 AREVA Document 51-9234885-000, "Exelon Byron and Braidwood RVCH Original Material and Fabrication Review"

8.12 AREVA Drawing 02-9232823E-000, "Byron Units 1 and 2/Braidwood Units 1 and 2 CRDM, Spare, & RVLIS Penetration Modification"

APPENDIX A: VERIFICATION OF SIF FOR CYLINDRICAL FLAW

This Appendix provides verification of the Excel macro KIeff_edge used to calculate the SIF intensity factor for the cylindrical flaw which considers plasticity correction. The test case considered in this Appendix used $a_o = 0.05$ inch, t = 0.5 inch, a/l = 0, and $\sigma_y = 41.45$ ksi.

Basis: Analysis of Flaws, 2001 through 2003 Addenda ASME Code, Section XI, Appendix A, Reference [8.1]

$K_I = [\ A_0\ G_0 + A_1\ G_1 + A_2\ G_2 + A_3\ G_3\ ]\ \sqrt{(\pi a/Q)}$

where $Q = 1 + 4.593\ (a/l)^{1.65} - q_y$

and $qy = [\ (A_0\ G_0 + A_1\ G_1 + A_2\ G_2 + A_3\ G_3) / \sigma_y\ ]^2 / 6$

For $a/l = 0.0$ (continuous flaw)

$a/t \leq 0.1$

$G_0 = 1.195$

$G_1 = 0.773$

$G_2 = 0.600$

$G_3 = 0.501$

Stresses are described by a third order polynomial fit over the flaw depth,

$S(x) = A_0 + A_1(x/a) + A_2(x/a)^2 + A_3(x/a)^3$

For the following given residual and transient stresses:

Wall Position, x (in)	Residual Stress (ksi)	Transient Stress (ksi)	Total Stresses (ksi)
0.000	12.73	0.132	12.859
0.042	14.70	0.131	14.826
0.083	16.66	0.129	16.792
0.125	16.48	0.127	16.603
0.167	16.29	0.123	16.412
0.208	16.13	0.118	16.248
0.250	15.97	0.116	16.082
0.283	17.28	0.104	17.382
0.333	18.59	0.092	18.678
0.375	17.08	0.078	17.157
0.417	15.57	0.043	15.615
0.458	28.48	-0.029	28.453
0.500	41.39	-0.2940	41.100

Stress over crack face:

x/a	x	Interpolated Stress (ksi)		
0.00	0.000	12.859	A_3 =	0.048207
0.10	0.005	13.093	A_2 =	-0.05433
0.20	0.010	13.327	A_1 =	2.356546
0.30	0.015	13.562	A_0 =	12.85844
0.40	0.020	13.796		
0.50	0.025	14.030		
0.60	0.030	14.264		
0.70	0.035	14.498		
0.80	0.040	14.732		
0.90	0.045	14.970		
1.00	0.050	15.210		
Plasticity Correction		$q_y = [(A_0G_0 + A_1G_1 + A_2G_2 + A_3G_3)/\sigma_y]^2 / 6$ =		0.029
		$Q = 1 + 4.593\ (a/l)^{1.65} - q_y$ =		0.971
		$K_I = [A_0G_0 + A_1G_1 + A_2G_2 + A_3G_3]\ \sqrt{(\pi a/Q)}$ =		6.906
		KIeff_edge =		6.906
		Difference =		0.0%